


SEC1A is a major Arabidopsis Sec1/Munc18 gene in vesicle trafficking during pollen tube tip growth

Steven Beuder^{1,†}, Cecilia Lara-Mondragón^{1,†}, Alexandria Dorchak and Cora A. MacAlister^{*} 

Department of Molecular, Cellular and Developmental Biology, University of Michigan, Ann Arbor, MI, USA

Received 21 September 2021; revised 22 February 2022; accepted 14 March 2022; published online 20 March 2022.

^{*}For correspondence (e-mail macalister@umich.edu).

[†]These authors are contributed equally to this study.

SUMMARY

Pollen tubes (PTs) grow by the targeted secretion of new cell wall material to their expanding tip region. Sec1/Munc18 (SM) proteins promote membrane fusion through regulation of the SNARE complex. We have previously shown that disruption of protein glycosylation in the *Arabidopsis thaliana* *hpat1 hpat3* double mutant leads to PT growth defects that can be suppressed by reducing secretion. Here, we identified five point mutant alleles of the SM protein *SEC1A* as *hpat1/3* suppressors. The suppressors increased seed set, reduced PT growth defects and reduced the rate of glycoprotein secretion. In the absence of the *hpat* mutations, *sec1a* reduced pollen germination and PT elongation producing shorter and wider PTs. Consistent with a defect in membrane fusion, *sec1a* PTs accumulated secretory vesicles. Though *sec1a* had significantly reduced male transmission, homozygous *sec1a* plants maintained full seed set, demonstrating that *SEC1A* was ultimately dispensable for pollen fertility. However, when combined with a mutation in another *SEC1*-like SM gene, *keule*, pollen fertility was totally abolished. Mutation in *sec1b*, the final member of the Arabidopsis SEC1 clade, did not enhance the *sec1a* phenotype. Thus, *SEC1A* is the major SM protein promoting pollen germination and tube elongation, but in its absence *KEULE* can partially supply this activity. When we examined the expression of the SM protein family in other species for which pollen expression data were available, we found that at least one Sec1-like protein was highly expressed in pollen samples, suggesting a conserved role in pollen fertility in other species.

Keywords: cell wall, secretory pathway, pollen, reproduction, glycosylation.

INTRODUCTION

Pollen tubes (PTs) grow by a highly polarized secretion mechanism known as tip growth. New cell wall and plasma membrane material are delivered by the fusion of Golgi-derived secretory vesicles at the growing PT tip. The cell wall overlaying the tip region has a specialized composition that allows for continued expansion while the shaft cell wall is reinforced and non-extensible (Cascallares et al., 2020). The vesicle trafficking required to sustain growth requires the participation of multiple protein complexes to target and tether vesicles to the proper membrane location and to drive membrane fusion. The assembly of the exocyst complex is a major mechanism of vesicle tethering, and several exocyst members have been shown to play important roles in pollen germination and PT growth (Cole et al., 2005; Hála et al., 2008; Bloch et al., 2016; Li et al., 2017; Beuder et al., 2020; Marković et al., 2020). Membrane fusion is driven by the SNARE (soluble N-ethylmaleimide-sensitive factor attachment

protein receptors) complex (Han et al., 2017). SNARE proteins are classified based on conserved amino acids into R-SNAREs that are generally associated with vesicles, and Q-SNAREs that are generally associated with the target membrane. Q-SNAREs are further divided into Qa, Qb and Qc SNAREs (Baker & Hughson, 2016). The force required for membrane fusion is hypothesized to derive from the ‘zippering’ of the SNARE complex from a *trans* form into a *cis* form bringing the two membranes into close proximity for fusion (Cascallares et al., 2020). Several Arabidopsis SNARE proteins have demonstrated roles in PT growth, in particular a group of Qa-SNAREs, also known as the Syntaxin of Plants (SYP) family (Sanderfoot et al., 2000). SYP124, SYP125 and SYP131 are partially redundantly required for pollen fertility (Slane et al., 2017).

The SNAREs are regulated by several families of proteins, a particularly important group of regulators is the Sec1/Munc18 (SM) family, which regulate SNARE complex assembly through physical interaction with Qa-SNAREs

and assembling *trans*-SNARE complexes (Südhof & Rothman, 2009). The Arabidopsis SM family contains three Sec1p orthologs, KEULE = SEC11, SEC1B and SEC1A (Assaad et al., 2001). KEULE is important for the formation of the cell plate during cytokinesis, through its interaction with the Qa-SNARE KNOLLE = SYP111 (Park et al., 2012), and as a general secretion factor through interaction with SYP121 and SYP132 (Karnik et al., 2013; Karnahl et al., 2018). KEULE is also required along with SEC1B for production of viable male and female gametophytes (Karnahl et al., 2018). No function has been previously described for SEC1A.

We have previously found that loss of function mutations in two exocyst complex members, *exo70a2* and *sec15a*, suppress PT growth defects of Arabidopsis *hydroxyproline O-arabinosyltransferases1 (hpat1) hpat3* double mutants (*hpat1/3* for brevity). The HPAT enzyme family catalyzes the first dedicated step in the production of a plant-specific post-translational protein modification, hydroxyproline *O*-arabinylation (Hyp-ara), which occurs abundantly on cell-wall-associated structural proteins of the Extensin (EXT) family, and are predicted to occur on proteins containing EXT-like domains in addition to secreted peptides of the CLE (CLAVATA3/Embryo Surrounding Region-Related) family (Ogawa-Ohnishi et al., 2013; Petersen et al., 2021). Hyp-ara is particularly important during PT growth; *hpat1/3* plants have reduced seed set due to PT defects including frequent tube rupture, slow PT growth and the initiation of secondary, sub-apical tips (MacAlister et al., 2016). In addition to the loss of Hyp-ara in the PT wall, *hpat1/3* PTs also have disrupted polarity of several major cell wall polymers including callose and the pectic polysaccharide homogalacturonan (Beuder et al., 2020). This loss of cell wall polarity is also associated with increased secretion of HPAT-modified glycoproteins. Reduced secretion in the exocyst mutants suppresses the pollen growth defects of *hpat1/3* and increases seed set. Thus, the *hpat1/3* genetic background is a convenient system for identification of novel PT secretion factors. Here we report the recovery of several mutant alleles of *sec1a* as suppressors of the *hpat1/3* pollen fertility defect.

RESULTS

sec1a mutants suppressed the *hpat1/3* fertility phenotype

Due to defects in PT growth, *hpat1/3* double mutants fertilize only a fraction of their available ovules, leading to low seed set and short siliques (MacAlister et al., 2016). We have previously described a mutagenesis screen in which we identified suppressors of the *hpat1/3* fertility defect (Beuder et al., 2020). Briefly, we chemically mutagenized *hpat1/3* seeds and in the M2 generation selected mutants with increased silique length and seed set. Following four generations of backcrossing, whole-genome sequencing

and data analysis as described in Beuder and MacAlister (2020), we identified candidate causative mutations. In addition to the previously reported mutants, we identified four unique mutations in the SM family member *sec1a*. These *sec1a* mutations included three glutamic acid to lysine missense mutations (E153K, E398K and E267K) and one truncation allele (W506stop; Tables S1–S4). Given the large number of *sec1a* alleles recovered, we performed direct sequencing of the SEC1A coding sequence in five additional suppressed lines. In one of these lines, we identified a fifth, threonine to isoleucine *sec1a* allele (T197I). All five suppressed lines displayed increased silique length and seed set relative to *hpat1/3* and had no other notable phenotypes (Figure 1a,b).

We confirmed the presence of all five *sec1a* alleles in the corresponding suppressor lines by polymerase chain reaction-based genotyping assays (Table S5). We further confirmed that the increased seed set phenotype cosegregated with the identified *sec1a* alleles in the fifth or sixth backcross F2 generations (Figure 1c). Segregation of the mutation was also distorted with a significant bias against recovery of homozygous wild-type (WT) SEC1A plants (Table 1), as expected for a mutation conferring a fertility advantage. Like the *exo70a2* and *sec15a hpat1/3* suppressors we previously reported (Beuder et al., 2020), both homozygous and heterozygous *sec1a* mutants displayed increased seed set, with homozygous mutants having a minor, but statistically significant increase in seed set beyond the heterozygous suppressors (Figure 1c). This behavior is consistent with a gametophytic increase of pollen fertility. We confirmed that the mutant pollen was responsible for suppression using reciprocal pollinations between the *sec1aw506* hpat1/3* suppressed line and the *hpat1/3* background strain. As expected, seed set was high when the suppressed line was used as the pollen parent, but set was low when *hpat1/3* pollen was used to fertilize either *hpat1/3* or *hpat1/3 sec1aw506** stigmas (Figure 1c).

The identified mutations occur broadly across the SEC1A coding sequence with mutations falling within domains 1, 2a, 3b and 2b (Figure 2a; Misura et al., 2000; Karnahl et al., 2018). The mutated residues were also conserved with the two other Arabidopsis SEC1 homologs, SEC1B and KEULE (Figure 2c). To better understand the potential consequences of these changes to protein structure, we used a homology modeling approach to fit the predicted Arabidopsis SEC1A protein sequence onto available protein structures (Kelley et al., 2015). The highest quality model, returned with a confidence score of 100.0, was the crystal structure of the Unc18 (Sec1)-syntaxin 1 complex from the choanoflagellate *Monosiga brevicollis* (Protein Data Bank identifier 2XHE; Burkhardt et al., 2011). The five mutations fell into two spatial clusters, one at the interface of domains 1 and 2A (E153 and T197) and the second where domains 2B, 3A and 3B approach (E267, E398 and

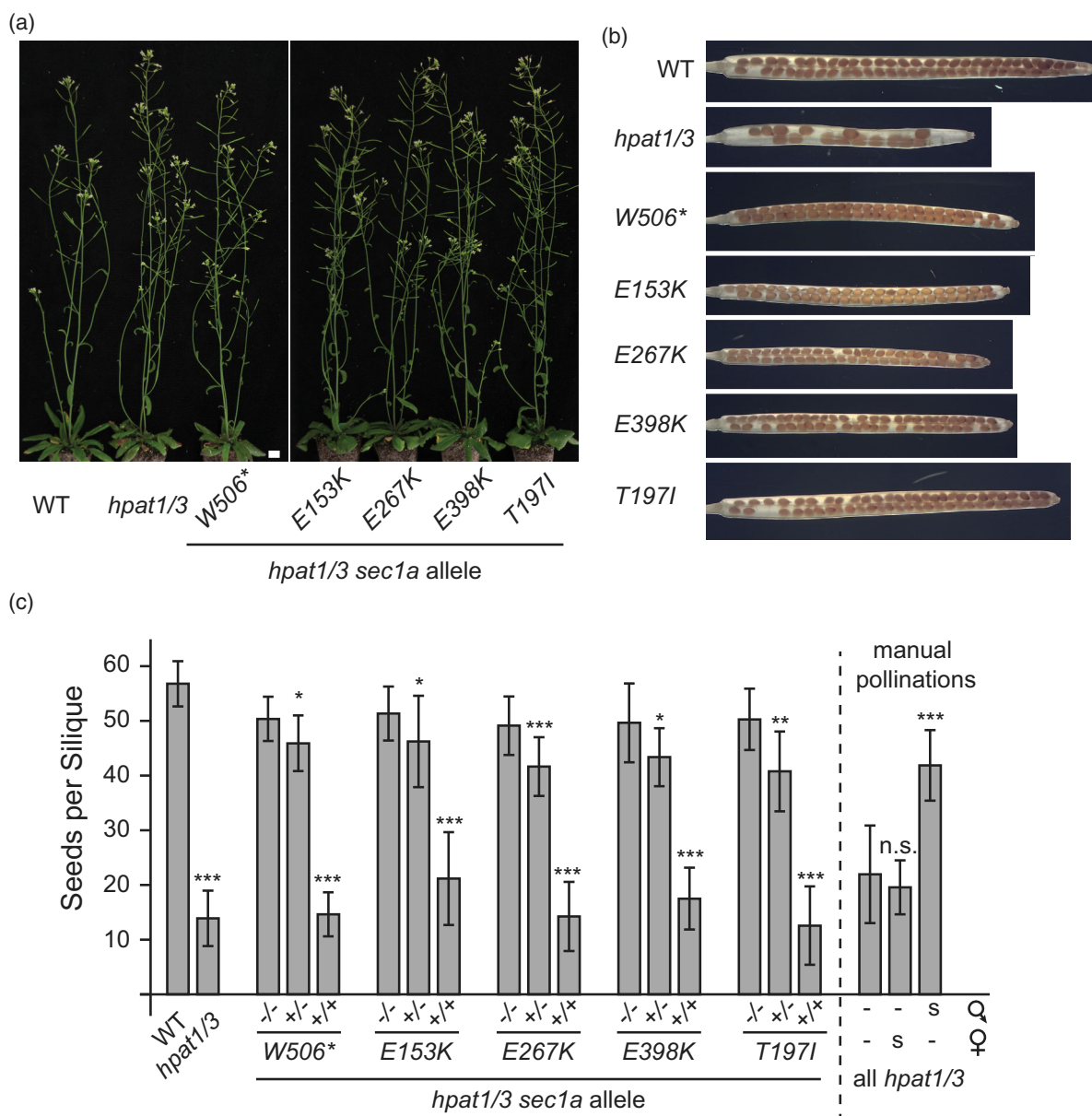


Figure 1. Mutations in *sec1a* increase seed set in the *hpat1/3* background.

(a) Plants of the indicated genotypes. Scale bar: 1 cm.

(b) Cleared nearly mature siliques of the indicated genotypes. All *sec1a* alleles are in the *hpat1/3* background. Long siliques are composite images.

(c) Average number of seeds per silique \pm standard deviation (SD). Bars to the left of the dashed line are self-pollinations while bars to the right are manual pollinations. *sec1a* segregating populations (BC5 or BC6 F2 generation) were grouped based on *sec1a* allele genotype. Statistical comparisons were made within sample groups (clustered bars). Stars indicate significance relative to the left-most bar in a group. Within the manual pollination group, 's' marks the suppressor (*hpat1/3 sec1aw506**), while '-' is the unsuppressed background strain (*hpat1/3*). Male parent is on the top row, female parent on the bottom. *Marks *t*-test *P*-value < 0.05, ***P* < 0.005; ****P* < 0.0005.

W506). The W506 truncation allele removes about one-third of the protein sequence including the majority of domain 2B (Figure 2b). The position of the mutations and the nature of the amino acid changes suggested possible protein folding defects and loss of protein function.

In order to confirm that suppression was caused by loss of SEC1A function in each suppressed line, we performed a transgenic rescue assay using a 5.3-kb fragment of the

WT genomic SEC1A sequence. Because the suppressive mutations increase pollen fertility, 'rescue' will reduce pollen fertility back to the level of the *hpat1/3* genetic background. Consequently, we predicted that pollen carrying a functional SEC1A transgene would be largely outcompeted by non-transgenic suppressed pollen. We transformed homozygous *hpat1/3 sec1a* mutant lines of all five alleles with the rescue construct. In the T1 generation, we

Table 1 Segregation ratio of *sec1a* mutant alleles in the *hpat1/3* background in the BC5 or BC6 generation

Allele	+/+	+/-	-/-	P-value
<i>sec1a-W506*</i>	13%	46%	42%	0.001704
<i>sec1a-E153K</i>	6%	58%	36%	0.000443
<i>sec1a-E267K</i>	3%	63%	35%	6.79E-05
<i>sec1a-E398K</i>	11%	44%	44%	0.000215
<i>sec1a-T1971</i>	3%	58%	39%	3.08E-05

$N = 72$ plants for each allele, P -value is calculated by the χ^2 test compared with the expected value for Mendelian segregation (25%/50%/25%).

performed reciprocal crosses with WT to determine male and female transgene transmission efficiency. In three independent T1s for each of the five *sec1a* alleles, we found that transgene transmission through the male was significantly reduced (~10–20% of progeny inherited the transgene), while inheritance through the female was not significantly different from the expected 50% (Figure S1), thus confirming that the suppressive phenotype was due to a loss of *SEC1A* function that was complemented by the *SEC1A* transgene in all five lines.

While our screen identified multiple single-nucleotide polymorphism alleles of *sec1a*, the publicly available T-DNA and transposon-insertion mutant collections did not provide promising candidate *SEC1A* mutants (Sessions et al., 2002; Alonso et al., 2003; Rosso et al., 2003; Woody et al., 2007; Kleinboelting et al., 2012). Indeed, it has been previously reported that *SEC1A* is one of only three genes within a 425-kb region of chromosome 1 lacking any coding region insertions (Borsics et al., 2006). Given that all five suppressor alleles are indistinguishable based on their increased seed set phenotypes and all were rescued by the WT transgene, we chose *sec1aW506** (hereafter *sec1a-1*) as the reference allele for further study.

***sec1a-1* partially suppressed *hpat1/3* PT defects and reduced glycoprotein secretion**

To better understand the nature of the *sec1a* effect on *hpat1/3* pollen fertility, we examined PTs directly. *hpat1/3* pollen exhibit a number of growth and morphological defects contributing to their low fertility, including reduced pollen germination, high rates of PT rupture, the initiation of sub-apical secondary tips ('branching') and reduced rates of elongation leading to an overall reduction in PT length (MacAlister et al., 2016; Beuder et al., 2020). While we found that the frequency of successful *sec1a-1 hpat1/3* pollen germination was not altered compared with the *hpat1/3* background, most other *hpat1/3* defects were partially suppressed (Figure 3). The incidence of PT branching, and rupture were both significantly reduced, although not to the level of WT pollen (Figure 3d,e). After 4 h of *in vitro* growth, we also found that the length of *sec1a-1 hpat1/3* PTs was

significantly increased compared with those of *hpat1/3* but, again, the suppressed PTs were still significantly shorter than those of WT (Figure 3b). Consistent with this increase in PT length, we also observed increased elongation rates in suppressed PTs (Figure 3f). Finally, we also noted a novel increase in PT width in the *sec1a-1 hpat1/3* mutants, an effect we had not observed for the exocyst-based suppressors of *hpat1/3* (Figure 3g; Beuder et al., 2020).

Given the status of *SEC1A* as an SM protein and its potential role in membrane fusion combined with our previous observation that reduced rates of secretion can suppress the *hpat1/3* phenotype, we hypothesized that *sec1a* may function through a similar mechanism. We have previously developed an assay to measure the rate of secretion of HPAT-modified proteins using a reporter protein composed of the EXT3 signal peptide fused to green fluorescent protein (GFP) with an internally inserted EXT3 glycosylation motif [GF(EXT3)P], expressed using the pollen-expressed *Lat52* promoter (Bate & Twell, 1998). The protein is Hyp *O*-arabinosylated in an HPAT-dependent fashion and is secreted at a higher rate in *hpat1/3* PTs compared with WT PTs (Beuder et al., 2020). We crossed this construct into WT, *hpat1/3* and *hpat1/3 sec1a-1* plants. A non-secretory pollen-expressed GFP (*Lat52::GFP*) was used as a control. *In vitro* grown PTs expressing the reporter were plasmolyzed by transfer to high-sucrose pollen germination media. We then measured the fluorescence intensity in the vacated cell wall area at the PT tip as well as the cytoplasmic signal. The 'secretion index' was calculated as the ratio of the fluorescence intensity in the cell wall fraction to that of the cytoplasmic fraction, normalized to background signal. Consistent with previous results, we found that the secretion index was significantly higher in *hpat1/3* pollen compared with WT, and it was reduced in the *sec1a-1* suppressor compared with the *hpat1/3* background, indicating that the rate of secretion of glycoproteins is reduced in the suppressed line (Figure 3h).

Given the altered secretion of HPAT-targeted glycoproteins, we hypothesized that endomembrane trafficking in general may be disrupted. To test this, we examined the distribution of vesicles in WT, *hpat1/3* and *hpat1/3 sec1a-1* PTs using the amphiphilic fluorescent dye FM4-64. The dye binds to the plasma membrane and is taken up through endocytosis. Within a few minutes it marks vesicles in a characteristic cone-shaped pattern in the 'clear zone' near the PT tip (Parton et al., 2001; Hepler & Winship, 2014). In WT tubes, we observed the expected pattern (Figure 3i). We found that the accumulation of vesicles at the PT tip was reduced in *hpat1/3* tubes relative to WT. We quantified this effect by measuring the fluorescence at the tip and normalizing it against the fluorescence intensity at a distal portion of the PT. We found that this ratio was significantly lower in the *hpat1/3* PTs (Figure 3j), consistent with increased secretory vesicle delivery leading to reduced

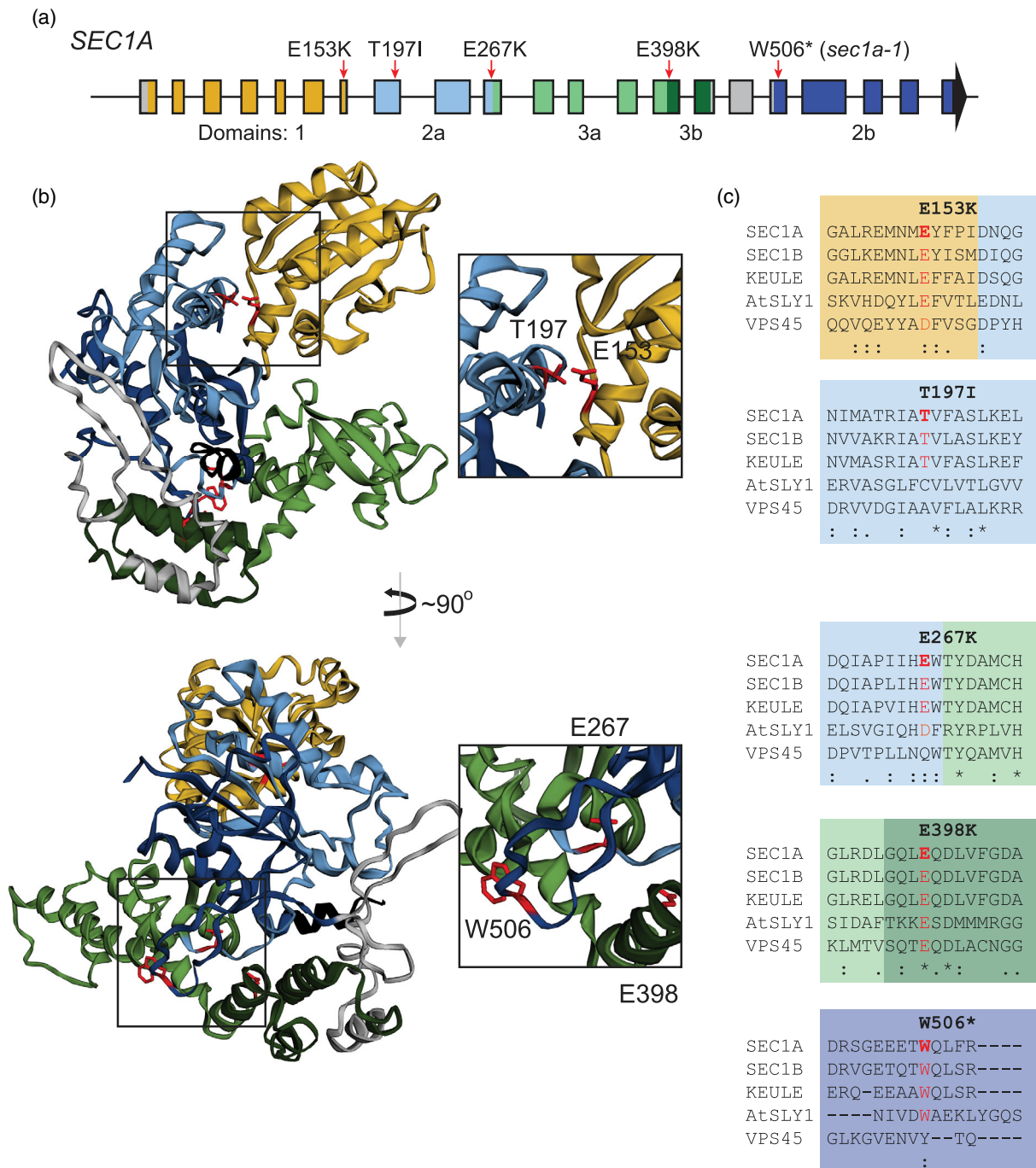
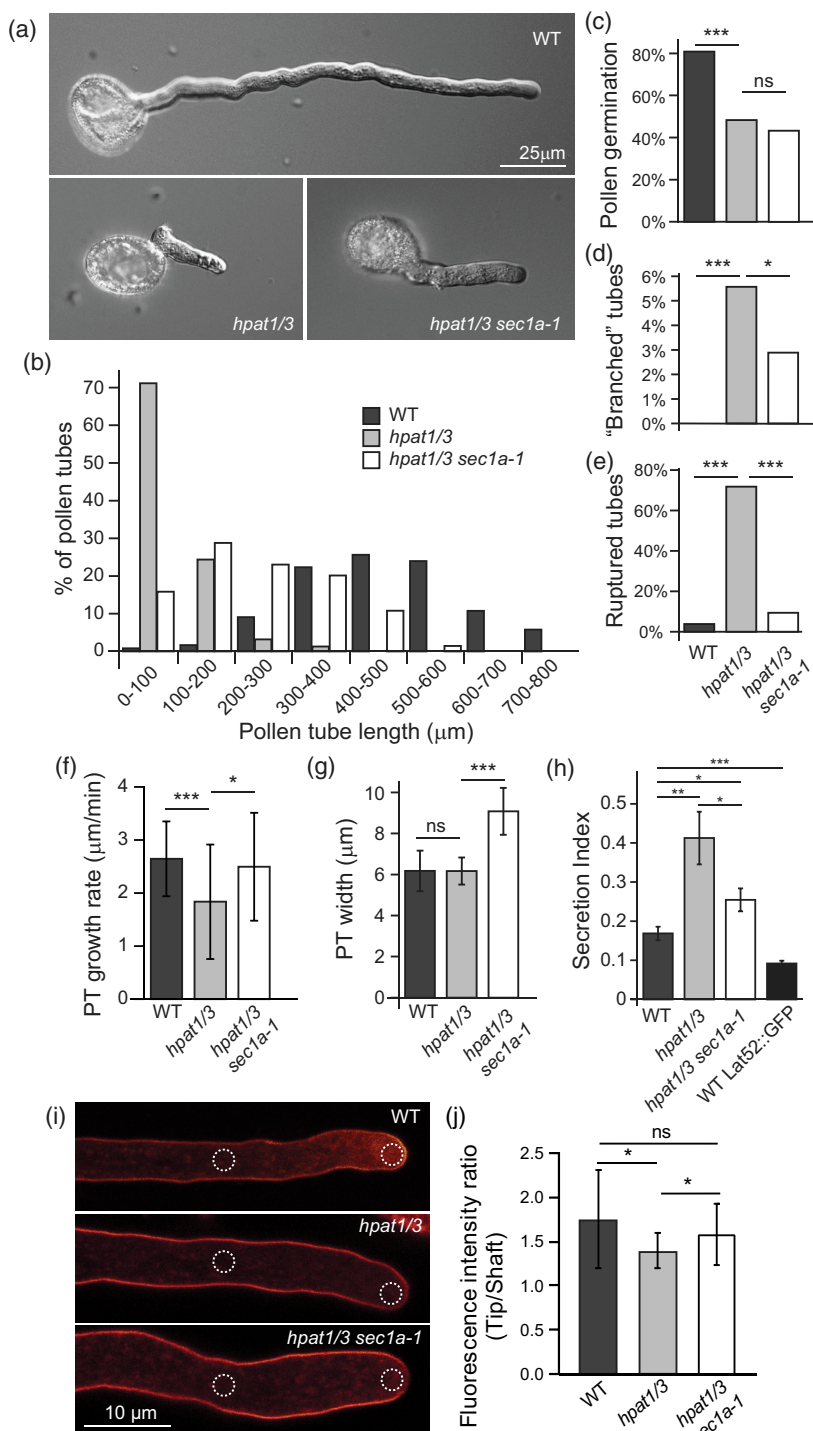


Figure 2. *sec1a* mutations occur in two clusters.

(a) The *SEC1A* locus structure with rectangles indicating exons. The positions of the identified mutations are marked with red arrows and the portions encoding the domains are colored as follows: domain 1, yellow; domain 2a, light blue; domain 3a, light green; domain 3b, dark green; and domain 2b, dark blue. Sequence not falling into a given domain is gray and the C-terminal tail is in black (Bracher et al., 2000; Karnahl et al., 2018).

(b) The homology model structure of the predicted Arabidopsis SEC1A protein sequence modeled onto the crystal structure of UNC18 (Sec1) of the choanoflagellate *Monosiga brevicollis* (Burkhardt et al., 2011). Domains are colored as in (a), and mutated residues and their side-chains are marked in red and labeled. The upper view shows the first cluster of mutations (E153 and T197) occurring at the interface between domain 1 and domain 2a, and the lower view shows an approximately 90° rotation along the vertical axis showing the second mutational cluster (W506, E267 and E398).

(c) Protein sequence alignments of the Arabidopsis Sec1/Munc18 (SM) proteins for the region of the five *sec1a* point mutations. The altered residue is marked in red if it is conserved between SEC1A and other sequences, and marked in orange if amino acid character is maintained.



secretory vesicle residence at the PT tip. As with the secretion index measured above (Figure 3h), this was also suppressed in the *hpat1/3 sec1a-1* PTs, where the normalized fluorescence intensity at the tip region was not significantly different from that of WT (Figure 3h).

***sec1a* pollen fertility was compromised and PTs accumulated secretory vesicles**

Pollen tube elongation is based on secretion. If SEC1A is acting as an SM protein contributing to SNARE complex assembly in PTs, we predicted PT growth would be

Figure 3. *sec1a* partially suppresses *hpat1/3* pollen phenotypes.

(a) Representative *in vitro* grown pollen tubes (PTs) of the indicated genotypes.

(b) Histogram of PT length after 4 h of *in vitro* growth. $N \geq 121$ PTs per genotype. The mean value for each genotype was significantly different from the others (*t*-test P -value < 0.0005).

(c) Pollen germination frequency after 2.5 h of *in vitro* growth ($N \geq 350$ pollen grains per genotype).

(d) Incidence of branched PTs after 2.5 h of *in vitro* growth ($N \geq 500$ PTs per genotype).

(e) Incidence of PT rupture after 2.5 h of *in vitro* growth ($N \geq 250$).

(f) Sustained growth rates of PTs were measured by the total change in length over a given period of time (~ 25 min) divided by the time interval in minutes ($N \geq 30$).

(g) PT width ($N \geq 30$).

(h) The secretion index measured for an HPAT-modified reporter protein [Lat52::GF(EXT3)P] expressed in PTs. Pollen was grown *in vitro* and transferred to high-sucrose media to trigger plasmolysis. The secretion index is the ratio of the fluorescence signal in the vacated portion of the PT (the cell wall area) divided by the fluorescence intensity in the cytoplasmic portion of the tube, normalized to background. Lat52::GFP is a control construct lacking a signal peptide or glycosylation sequence and is included as a control (mean \pm SE; $N > 28$; asterisks mark significant differences, **t*-test $P < 0.05$, ** $P < 0.005$; *** $P < 0.0005$).

(i) PTs of the indicated genotype stained with FM4-64 to mark vesicles. The two regions of interest from which fluorescence intensity measures (mean gray value) were taken are circled.

(j) Fluorescence quantification of the tip region normalized to the fluorescence in the shaft [mean \pm SD wild-type (WT) $N = 16$, *hpat1/3* $N = 20$ and *hpat1/3 sec1a-1* $N = 22$; *marks significant differences, *t*-test $P < 0.05$].

compromised in *sec1a* mutants in the absence of the *hpat1/3* mutations. To test this prediction, we outcrossed *sec1a-1* and the four other *sec1a* alleles to WT. After fixing for the WT *HPAT1* and *HPAT3* alleles, we measured seed set in segregating families based on *sec1a* genotype. We found no statistically significant difference in seed set between the *sec1a* homozygous mutants and sibling WT or heterozygous plants (Figure S2), suggesting that mutant pollen remains viable and competent to fertilize *in vivo*. A more sensitive measure of pollen fertility is the relative success of mutant and WT pollen when in competition for a limited number of ovules. Therefore, we performed transmission rate tests with *sec1a-1/+* parents. For female transmission of the mutant allele, we found no significant deviation from the expected value (49% heterozygous progeny, $N = 92$, χ^2 P -value = 0.834). However, the male transmission of the mutant allele was significantly reduced (1.46% heterozygous progeny, $N = 137$, χ^2 P -value = 6.39×10^{-30}), demonstrating a fitness cost to mutant pollen.

We next compared PTs directly during *in vitro* growth. After 1 h in pollen growth media, we found that fewer *sec1a-1* pollen had successfully germinated (61.0%, $N = 6130$) compared with WT (91.3%, $N = 3890$). We next measured PT length and width of *sec1a-1* and WT PTs, and found a reduction in average PT length and an increase in PT width in *sec1a-1* (Figure 4c,d). Consistent with reduced PT lengths, the rate of PT elongation was also reduced in *sec1a-1* versus WT (Figure 4e). We also measured rates of PT rupture and branching, two phenotypes characteristic of *hpat1/3*, which *sec1a-1* partially suppressed (Figure 3d,e). We found no change in either the incidence of PT rupture (WT = 2.23%, $N = 269$; *sec1a-1* = 2.02%, $N = 247$; χ^2 P -value = 0.826) or in the initiation of secondary tips (WT = 0.7%, $N = 285$; *sec1a-1* = 0.35%, $N = 285$; χ^2 P -value = 0.478) after 2.5 h of *in vitro* growth. Thus, *sec1a-1* pollen germinated less frequently and PTs elongated more slowly but, aside from an increase in PT width, the PTs were morphologically normal (Figure 4a,b).

To better understand the *in vivo* behavior of the *sec1a-1* PTs and to potentially account for the full seed set of the mutants, we used an *in vivo* imaging approach to follow PT growth in the pistil. Given the lower rate of PT elongation observed *in vitro*, we predicted that the *sec1a-1* PTs would penetrate the pistil more slowly than WT PTs. We stained WT pistils 8 h after pollination with either WT or *sec1a-1* pollen using Aniline blue fluorochrome, a callose-binding dye that binds the callose-rich PT cell walls (Mori et al., 2006). We observed that WT pollen had largely traversed the pistil at this time (Figure 4f), while *sec1a-1* pollen was noticeably less advanced within the female tissue (Figure 4g). Thus, the slower rate of *sec1a-1* PT growth *in vivo* likely leads to reduced competitiveness against the faster WT pollen. Although slower growing, the *sec1a-1* pollen was still competent to fertilize, leading to full seed set in the homozygous mutants (Figure S2).

If SEC1A is involved in vesicle trafficking, as would be predicted for an SM protein, we would expect the distribution of secretory vesicles might be altered in *sec1a* PTs. To test this, we used a secretory vesicle-specific marker, the Rab GTPase, RabA4B fused to the fluorescent protein mRuby2 to compare the distribution of secretory vesicles in *sec1a-1* and WT PTs (Preuss et al., 2004; Lam et al., 2012). We observed the expected pattern in WT PTs, specifically a cone-shaped population of secretory vesicles at the PT tip, but when we crossed this reporter into the *sec1a-1* background, we noted an increase in the total fluorescence intensity within the PT (Figure 4h–j), which was consistent with an accumulation of secretory vesicles, potentially due to reduced rates of vesicle fusion in the *sec1a* mutants, consistent with what we had previously observed using FM4-64 to mark vesicles in the *hpat1/3* background (Figure 3i,j).

SEC1A localization

Available mRNA sequencing data indicate that *SEC1A* is expressed primarily, if not exclusively, in pre-anthesis anthers, in open flowers containing pollen and in purified pollen (Loraine et al., 2013; Klepikova et al., 2016). Proteomic data further support the pollen expression of *SEC1A* (Grobei et al., 2009). To determine the subcellular localization of *SEC1A*, we generated a fluorescent reporter line consisting of 664 bp of *SEC1A* promoter sequence, the full coding region and a C-terminal fusion with the fluorescent protein mNeonGreen (*SEC1A-mNG*; Figure 5a). We transformed this construct into WT and *sec1a-1* plants. To test for functionality of the fusion protein, we performed reciprocal crosses between the *sec1a-1* *SEC1A-mNG* T1s and WT. Given that *sec1a-1* significantly reduced pollen transmission, a functional transgene should increase fertility and confer a transmission advantage to transgenic pollen compared with non-transgenic sibling pollen. In three independent *sec1a-1* T1s we found elevated transmission of the *SEC1A-mNG* transgene through the male (~85% of progeny inheriting the transgene, $N \geq 89$), while female transmission was unaffected (50% progeny inheriting the transgene, $N \geq 83$; Figure 5b), confirming that the fusion construct was functional.

We examined the localization of the reporter in *in vitro* grown PTs and observed diffuse, cytoplasmic fluorescence near the tip of the PT (Figure 5c). Because Arabidopsis PT growth is oscillatory (Damineli et al., 2017), we confirmed that PTs maintained this pattern of localization during active growth by following individual tubes over time (Figure 5d).

SEC1A and KEULE are redundantly essential for pollen fertility

Although the male transmission efficiency of the *sec1a-1* allele was significantly reduced in the absence of the

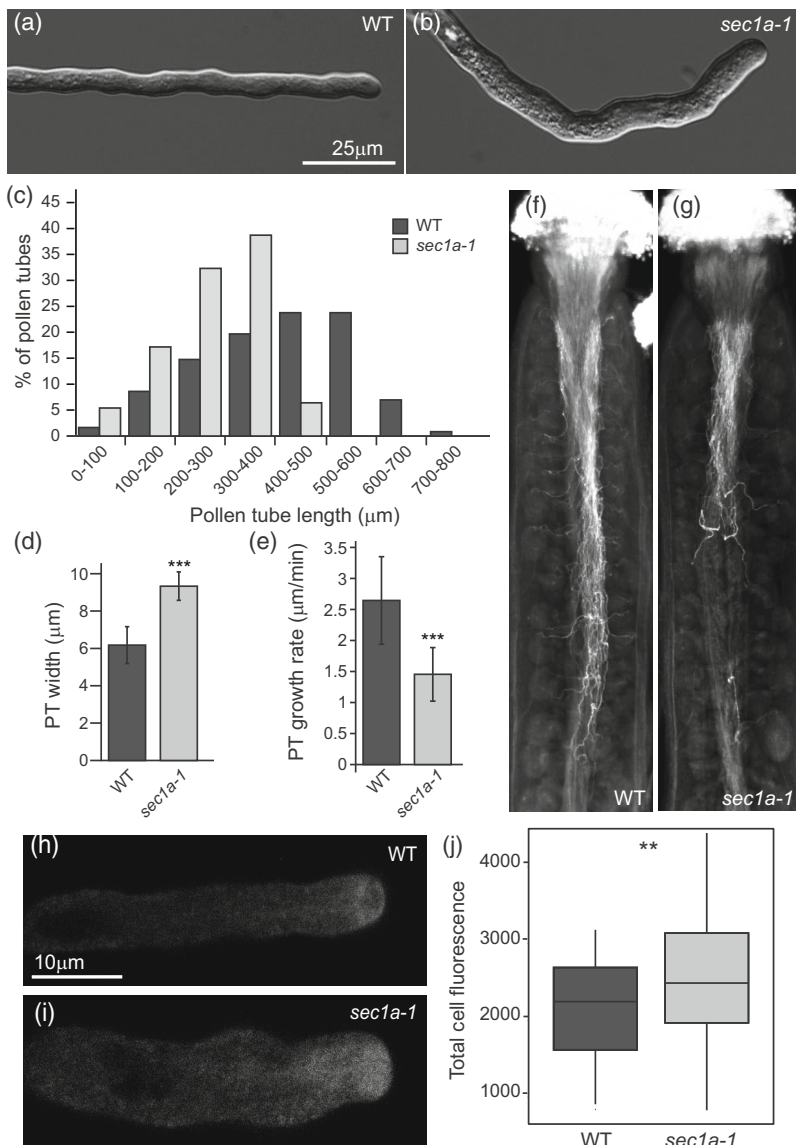


Figure 4. *sec1a* single mutants reduce pollen fertility.

Representative *in vitro* grown wild-type (WT) (a) and *sec1a-1* (b) pollen tubes (PTs).

(c) Histogram of PT length after 4 h of growth ($N \geq 240$ PTs per genotype).

(d) Mean PT width (\pm SD, $N \geq 30$, ***marks *t*-test $P < 0.00005$).

(e) Mean sustained PT growth rate (\pm SD, $N \geq 30$, ***marks *t*-test $P < 0.00005$).

(f, g) Aniline blue fluorochrome-stained WT pistils 8 h after pollination with the indicated genotype.

(h, i) The secretory vesicle marker Lat52::mRuby2-RabA4B expressed in WT (h) and *sec1a-1* (i) PTs.

(j) Quantification of RabA4B reporter fluorescence (**marks *t*-test $P \leq 0.0025$; WT $N = 53$ and *sec1a-1* $N = 75$).

hpat1/3 mutations, the ability of the homozygous *sec1a* mutants to achieve full seed set (Figure S2) suggested that *SEC1A* is ultimately dispensable for PT growth. Given the importance of secretion to PT growth and the importance of SM proteins to this process, we hypothesized other SM proteins may be functioning redundantly with *SEC1A*. The Arabidopsis genome encodes three Sec1p-like SM proteins; *SEC1A*, *SEC1B* and *KEULE* (*KEU/SEC11*; Sanderfoot et al., 2000; Assaad et al., 2001). *KEULE* has a well-described role in cytokinesis, functioning together with the SNARE protein *KNOLLE/SYP111* and, as a result, *keu* mutants are seedling lethal (Assaad et al., 1996). At the protein sequence level, the three share a minimum of 57.9% sequence identity and 71.9% sequence similarity. Furthermore, available mRNAseq expression data indicate that *SEC1A*, *SEC1B* and *KEULE* all achieve proportionally

high levels of expression in anthers, pre-anthesis (Figure 6a; Klepikova et al., 2016) and in mature pollen grains (Figure 6b; Loraine et al., 2013). Microarray expression data are also available for *SEC1B* and *KEULE*, and indicate high transcript levels in pollen samples with *SEC1B* also expressed during pollen development in the uninucleate microspore and bicellular pollen stages (Honys & Twell, 2004; Qin et al., 2009). Given their sequence similarity and partially overlapping expression patterns, we next tested for a potential contribution of *SEC1B* and *KEULE* to PT elongation.

To determine if either *SEC1B* or *KEULE* alone measurably contributed to pollen fertility, we tested the male and female transmission efficiency of insertional mutants in *sec1b* (Karnahl et al., 2018; GABI-KAT_601G09) and *keule* (GABI-KAT_513H06). We found no significant difference between the observed and expected transmission for either

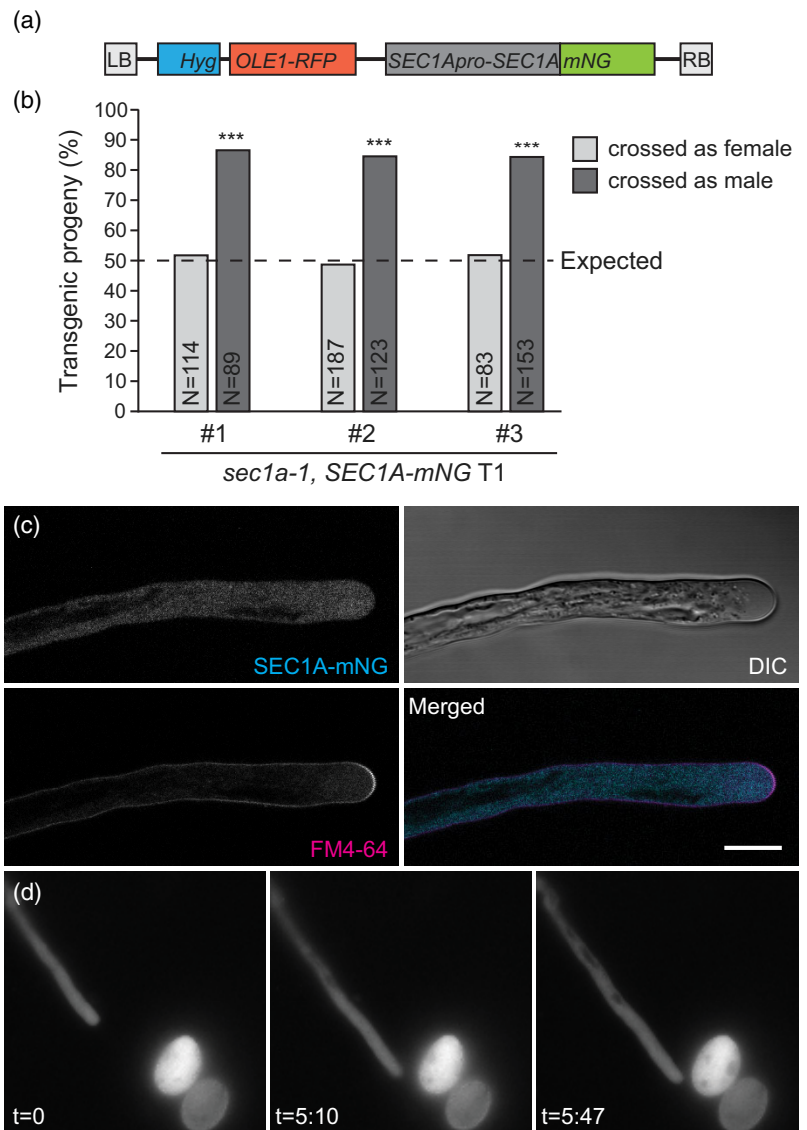
Figure 5. SEC1A localization.

(a) The structure of the SEC1A reporter construct including the *SEC1A* coding region under the native promoter fused to mNeonGreen and a selection cassette with Hygromycin resistance and a seed expressed RFP reporter (OLE1-RFP).

(b) The transgene rescues the *sec1a-1* low transmission efficiency. When crossed as a male, transgene-carrying pollen are more likely to fertilize than non-transgenic sibling pollen, while transmission through the female is not altered (***)marks χ^2 $P < 0.0005$, sample size is given in bars).

(c) Confocal image of SEC1A-mNG expression in representative wild-type (WT) pollen tube (PT) co-stained with FM4-64. Medial z-slice shown with individual channels and merged fluorescent channels. mNeonGreen signal is pseudo-colored cyan, FM4-64 is pseudo-colored magenta, and overlapping signals are white. Scale bar: 10 μ m.

(d) Sequential images of a single growing PT with time given relative to the start of imaging.



mutation through either the male or female (Figure S3d). As expected, we were unable to recover homozygous *keule* mutant plants from self-fertilized heterozygous plants ($N = 48$), and we observed the segregation of deformed seeds and seedlings with the previously described *keule* phenotype (Figure S3b,c; Assaad et al., 1996).

We next crossed *sec1b* and *keu*⁺ to *hpat1/3* to determine if these mutations could also suppress the *hpat1/3* pollen phenotypes as observed for *sec1a*. We observed no significant change in seed set in *hpat1/3* plants carrying the *sec1b* or *keule* mutations compared with sibling *hpat1/3* plants (Figure 6c). We also found no statistically significant deviation in male transmission for either *keu* or *sec1b* in this background (42% heterozygous progeny, $N = 88$ for *keule* and 50% heterozygous progeny, $N = 60$ for *sec1b*). Therefore, *sec1a* is unique in its ability to suppress the *hpat1/3* pollen defects.

To test for functional redundancy between these genes, we performed pairwise crosses between *sec1a-1* and *sec1b* and *keu*⁺. *sec1b* and *keu* have been previously shown to be redundantly required for gametophyte function with double mutant gametophytes displaying late-stage pollen grain abortion and non-viable ovules. Thus, populations segregating for *sec1b* and *keu* are limited to the segregation of, at most, double heterozygous plants (Karnahl et al., 2018). In contrast to the *sec1b* and *keu* combination, we recovered the double mutant between *sec1a-1* and *sec1b* and isolated *sec1a-1 keu*⁺ plants without undue difficulty. We found no notable vegetative phenotypes (Figure S3d). We also found no statistically significant differences in seed set with the exception of reduced seed set in the *keu*⁺ *sec1b*⁺ plants, consistent with their redundant requirement for ovule viability (Figure S3f).

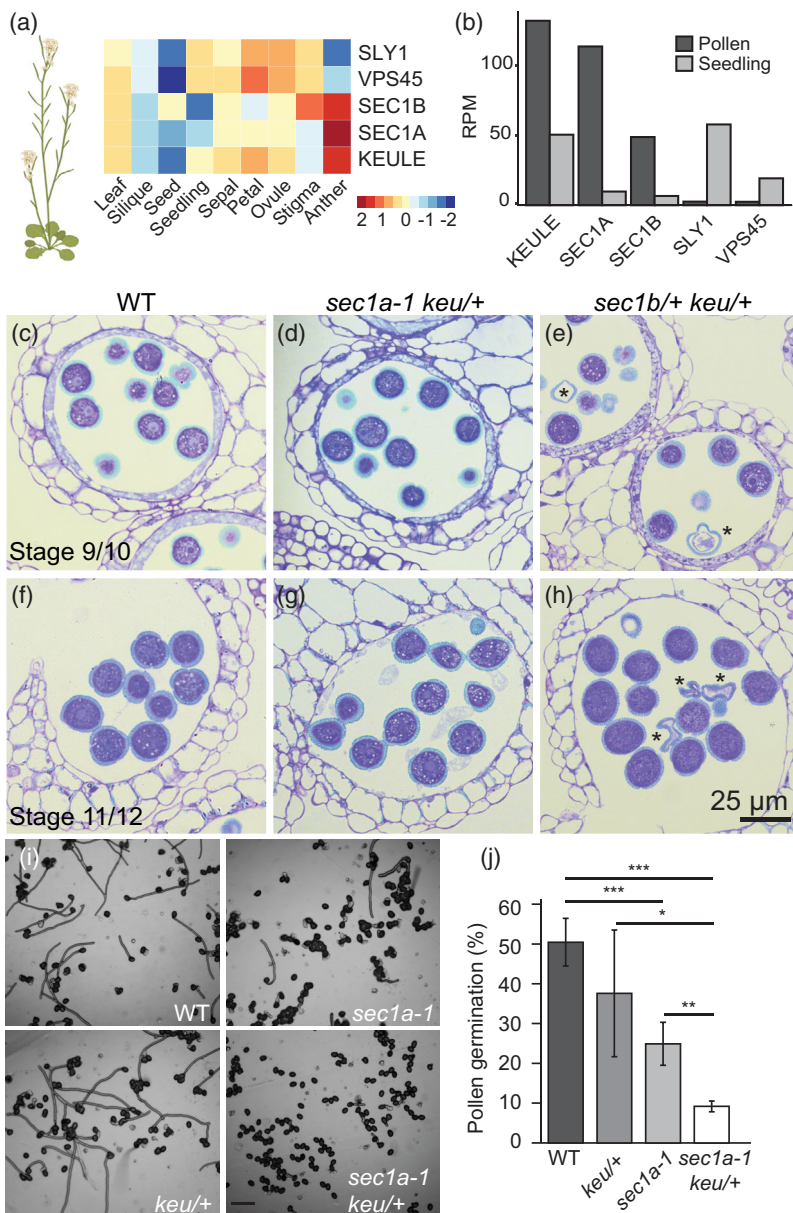


Figure 6. *SEC1A* and *KEU* are required for pollen germination. (a) Heatmap of the mRNA sequencing expression values of the indicated genes (Klepikova et al., 2016).

(b) Histogram of pollen and seedling mRNA sequencing data (Lorraine et al., 2013). All three *Sec1p*-like genes displayed high levels of expression in pollen and anthers.

(c-h) Toluidine blue-stained sections of developing anthers from stage 9 to 10 (c-e) or stage 11 to 12 (f-h) flower buds (Sanders et al., 1999). Both wild-type (WT) and *sec1a-1 keu/+* plants produce morphologically normal pollen, while *sec1b/+ keu/+* plants segregate for aborted pollen grains (marked with*).

(i) Pollen from plants of the indicated genotype after 2 h on *in vitro* pollen germination media.

(j) Quantification of pollen germination rate (mean \pm SD, five biological replicates of $N \geq 225$ per replicate). Asterisks mark significantly different *t*-test *P*-values (*** ≤ 0.0005 ; ** ≤ 0.005 ; * ≤ 0.05).

To test for functional redundancy with *sec1a-1* in pollen fertility, we fixed for the mutation in *sec1a-1* and monitored the segregation of *sec1b* and *keu* to compare single and double mutant pollen fertility. We found no statistically significant deviation in the expected 1:2:1 segregation ratio for *sec1b* in self-fertilized *sec1a-1 sec1b/+* progeny ($N = 34$). To more carefully test for a male transmission impact, we crossed these plants as males to WT and genotyped for the transmission of the *sec1b* mutant allele. We found no significant change in *sec1b* transmission compared with the expected value (42% *sec1b/+* progeny, $N = 84$, $\chi^2 P$ -value = 0.12663). For the segregation of *sec1a keu/+* plants, we expected the homozygous *keu* plants not to survive until genotypeable age and therefore expected a

1:2 segregation ratio (WT:*keu/+*). However, the *keu* mutation segregation was closer to a 1:1 ratio ($N = 48$; 25 WT, 23 *keu/+*), suggesting a gametophytic transmission defect. When we tested the male transmission of *sec1a keu/+* plants we found *keule* transmission was fully abolished (0 *keule/+* progeny, $N = 144$, $\chi^2 P$ -value = 3.55296×10^{-33} ; Figure S3g). Therefore, *SEC1A* and *KEU* are redundantly essential for male fertility.

sec1b/+ keu/+ plants have been previously reported to produce aborted pollen grains (Karnahl et al., 2018). Here, we find that *sec1a-1 keu* pollen phenotype to the previously described *sec1b keu* pollen abortion phenotype, we sectioned anthers from WT, *sec1a-1 keu/+* and *sec1b/+*

keu⁺ plants. We observed the segregation of aborted pollen grains in *sec1b*⁺ *keu*⁺ anthers from stages 9 through to maturity (Figure 6e,h). However, the pollen grains in *sec1a-1 keu*⁺ anthers were morphologically normal with no sign of abortion (Figure 6d,g), suggesting that the fertility defect in this genotype occurs later in pollen function. We next tested the impact of *keu* on the ability of *sec1a-1* pollen to germinate. While *sec1a-1* alone significantly reduced germination frequency compared with the WT, pollen from *sec1a-1 keu*⁺ plants had a significant further reduction compared with *sec1a-1* alone. Therefore, while both *SEC1A* and *SEC1B* interact with *KEU* in male fertility, *SEC1B* and *KEU* are required for pollen development while *SEC1A* and *KEU* are required for pollen germination.

SEC1A orthologs are highly expressed in pollen

The role of *SEC1A* and the other Arabidopsis SM proteins in pollen fertility next prompted us to investigate the evolutionary history of this gene family. The presence of a *SEC1B* ortholog is limited to a subgroup within the dicots (the Brassicales-Malvales clade), suggesting a relatively recent origin for *SEC1B* following the duplication of an ancestral *KEU*-like gene in this lineage. However, the divergence between *SEC1A* and *KEU* likely occurred after the evolution of angiosperms, but before the separation of the monocots and eudicots (Karnahl et al., 2018).

To explore the possible role of SEC1 proteins as a general feature of PT growth, we identified SM family members in species for which pollen expression data were available. We have recently published a transcriptomic data set for tomato (*Solanum lycopersicum*) reproductive tissues including pollen and PTs (Lara-Mondragón & MacAlister, 2021). Transcriptomic data were also available for rice, maize and the basal angiosperm *Amborella trichopoda* (Wei et al., 2010; Davidson et al., 2011; Flores-Tornero et al., 2020). We identified putative orthologs of the SM proteins in these species through sequence similarity searches using the Arabidopsis *SEC1A* protein as bait, and identified predicted SM proteins of the SEC1 clade as well as SLY1 and VPS45 members. VPS45 and SLY1 are implicated in vacuolar trafficking and endoplasmic reticulum (ER)-Golgi trafficking, respectively (Søgaard et al., 1994; Bassham & Raikhel, 1998; Zouhar et al., 2009). We found that the tomato *SEC1A* gene was split into two gene models (Soly-c01g091290 and Soly-c01g091300), corresponding to the first ~160 aa and the remainder of the protein. We consulted the available RNA sequence data to determine the appropriate exon distribution for a manually corrected gene model, labeled SISEC1A (Figure S4). The merged gene model produced a full-length SEC1-like protein.

We generated a maximum parsimony phylogenetic tree using the identified protein sequences along with the budding yeast Sec1p, Sly1p and VPS45p sequences. We found that the VPS45 and SLY1 sequences clustered into two

well-supported clades, generally with a single representative per species. The SEC1 clade, however, was more complex and, with the exception of the single SEC1 protein from *Amborella*, contained two or three members per species (Figure 6a). Within this limited sample of species, tomato was most similar to *Arabidopsis* in term of SEC1 genes with a clear AtSEC1A ortholog and a single sister to KEU and SEC1B. To better understand the expression pattern of the SM proteins, we generated heat maps of expression across vegetative and reproductive tissues. For tomato, we found that the pollen and PT samples were heavily enriched for expression of *SISEC1A*, while the other SM genes had depleted expression in the pollen samples. In our original analysis of the transcriptomic data, we had identified the second (larger) tomato *SEC1A* model as one of the 1229 tomato genes with enriched expression in pollen grain samples (Lara-Mondragón & MacAlister, 2021).

In the two monocots (rice and maize), we identified three SEC1-like proteins including a moderately well-supported sister group to the SEC1A clade containing one rice and maize gene. Interestingly, the maize gene in the SEC1A group (GRMZM5G830776) was highly expressed in anther and pollen samples, while the other SEC1-like genes had depleted transcript abundance in pollen. Of the three rice SEC1 genes, the two genes present on the microarray used in Wei et al. (2010) were both well expressed in pollen samples, particularly from the tricellular stage through PTs (Figure 7d). Finally, the single SEC1 gene from *Amborella* was also strongly expressed in pollen (Figure 7e). Therefore, in each species analyzed at least one SEC1-like gene had high expression in pollen samples. In *Amborella*, tomato and maize, this high expression was limited to one SEC1 gene, while in *Arabidopsis* and rice, multiple SEC1s had high pollen expression. Determining the functional significance of these expression patterns and these genes will require future work.

DISCUSSION

Here we demonstrate an important function for *SEC1A* during PT growth. *sec1a* mutant PTs had reduced germination and compromised tube growth rates leading to shorter tubes *in vitro* and *in vivo* and reduced pollen fitness (Figure 4). The likely cause of this slower growth, given that *SEC1A* encodes an SM protein, is the reduced secretion of vesicles, limiting cell expansion. Consistent with this hypothesis, we demonstrated accumulation of secretory vesicles in the mutant PTs (Figure 4h-j) and reduced secretion of a glycosylated reporter protein in the *hpat1/3 sec1a-1* suppressed line (Figure 3h). We have previously found reduced secretion resulting from mutation of the exocyst complex as a suppressive mechanism for the *hpat1/3* phenotype (Beuder et al., 2020). It is likely that the suppression by *sec1a* mutations follows a similar mechanism, although how specifically this occurs is unknown.

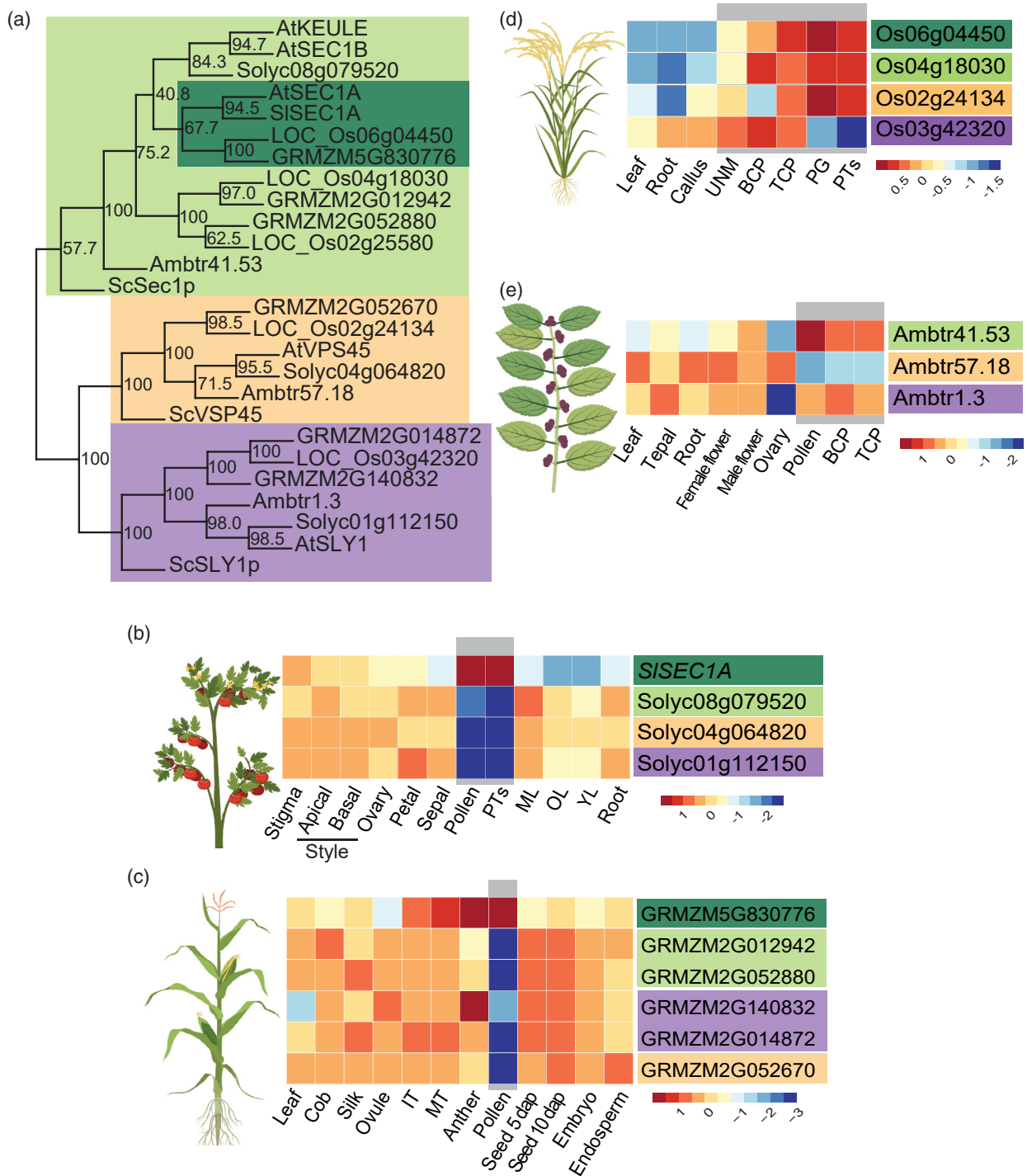


Figure 7. *SEC1* genes are highly expressed in pollen in other species. (a) Maximum parsimony phylogenetic tree with 100 replicate bootstrap values given in nodes. The VPS45 clade is marked in orange, the SLY1 clade is marked in purple, and the SEC1-like clade is marked in green with the SEC1A-like subclade marked in dark green. The protein sequence for *SISEC1A* was manually corrected to account for its split into two gene models (*Solyc01g091290* and *Solyc01g091300*; Figure S4). The *Amborella* gene names are given by scaffold and gene number. (b–e) Heatmaps corresponding to the log₂ of the mean expression values for the indicated genes based on available mRNA-seq or microarray data. (b) Tomato expression values (Lara-Mondragón & MacAlister, 2021). (c) Maize expression values (Davidson et al., 2011). (d) Rice expression values (Wei et al., 2010). (e) *Amborella trichopoda* expression values (Flores-Tornero et al., 2020). Pollen, pollen tube (PT) and developing pollen samples are marked with gray. PTs, pollen tubes; PG, pollen grains; UNM, uninucleate microspore; BCP, bicellular pollen; TCP, tricellular pollen; ML, mature leaf; OL, old leaf; YL, young leaf; IT, whole tassel 10 days before emergence; MT, whole tassel after emergence; dap, days after pollination.

Given that the HPATs are glycosyltransferases, we expect that the *hpat1/3* phenotype reflects the impact of the loss of hydroxyproline O-arabinoxylolation from the proteins that they modify. The largest known group of HPAT-modified proteins are the EXT cell wall structural proteins (Petersen et al., 2021). The EXTs form a cross-linked network and are hypothesized to serve as a scaffold for the assembly of pectin during cell wall formation (Cannon et al., 2008). Deglycosylated EXTs have reduced *in vitro* cross-linking ability, presumably compromising their ability to function as structural proteins (Chen et al., 2015). We hypothesize two possible ways in which reduced secretion may suppress the *hpat1/3* phenotypes. First, suppression may occur by slowing the delivery of new cell wall material to the PT tip, allowing the PT to compensate for the absence of hydroxyproline O-arabinoxylolation. In this way, reduced growth itself is the compensation mechanism. An alternative, though not mutually exclusive explanation, envisions the non-glycosylated HPAT-target proteins as 'toxic' to cell wall assembly. In the *hpat1/3* mutants, these non-modified proteins are secreted more quickly (Beuder et al., 2020; Figure 3h). Such proteins in the wall might interfere with wall stability, and by simply reducing their trafficking the wall can be restored. Determining the specific mechanism of suppression and identifying the specific HPAT target proteins mediating this process will require additional work.

Though we initially identified *sec1a* mutants based on suppression of the *hpat1/3* phenotype, we found that SEC1A is an important regulator of PT growth in its own right. SM proteins promote membrane fusion by regulating SNARE complex assembly through the binding of Qa-SNAREs or assembling *trans*-SNARE complexes (Baker & Hughson, 2016; Risselada & Mayer, 2020). Several SNARE proteins with functions in pollen have been identified (Sanderfoot et al., 2001; Slane et al., 2017; Sogawa et al., 2020; Rui et al., 2021). Of particular interest here are three Qa-SNAREs of the SYP family (SYP124, SYP125 and SYP131), which are all exclusively expressed in male gametophytes (Silva et al., 2010; Ichikawa et al., 2015; Slane et al., 2017). The three are redundantly required for male transmission, and *syp124/125/131* triple mutant PTs are shorter and wider than those of transgenically rescued sibling pollen (Slane et al., 2017). This phenotype is reminiscent of the PT phenotype we observed in the *sec1a* mutants (Figure 4), suggesting a possible mode of action for SEC1A through the binding of these three Qa-SNARE proteins or SNARE complexes containing them, though further work will be required to test this hypothesis.

The diffuse localization we observed for SEC1A-mNG in PTs (Figure 5c) was somewhat unexpected as SM proteins generally localize to the target membrane for vesicle fusion (Carr et al., 1999). In the case of tip-growing PTs, this would be the plasma membrane near the tip. The observation that the reporter construct rescues *sec1a*'s low

transmission phenotype indicates that the fusion protein is functional (Figure 5b). The PT localization of SEC1A-mNG was also consistent with the reported cytoplasmic localization of SEC1A when expressed under the KNOLLE promoter in roots (Karnahl et al., 2018). The localization of SYP124, SYP125 and SYP131 has been examined by several groups. SYP131 localizes primarily to the PT plasma membrane (Enami et al., 2008; Ichikawa et al., 2015). The localization of SYP124 and SYP125 is more complicated. They both display considerable cytoplasmic signal as well as some plasma membrane signal largely excluded from the tip at a distance that differs between SYP124 and SYP125 (Enami et al., 2008; Silva et al., 2010; UI-Rehman et al., 2011; Ichikawa et al., 2015; Slane et al., 2017). This difference in localization has been suggested to reflect a functional difference with SYP124 and SYP125 operating in the recycling pathway, while SYP131 operates in vesicle secretion (Ruan et al., 2021). The cytoplasmic SYP124 and SYP125 signal is similar to SEC1A-mNG's general localization to the cytoplasm and may reflect a functional relationship.

Though *sec1a* pollen had compromised fertility in transmission tests (Figure S3g), the homozygous mutant plants still achieved high seed set, indicating that SEC1A is ultimately dispensable for pollen function (Figure S2). However, we found fertility was fully abolished in the *sec1a keu* double mutant pollen, suggesting that, in the absence of SEC1A activity, KEU could partially substitute during PT growth. SEC1B on the other hand did not measurably contribute to the *sec1a* phenotype (Figure 6f). Interestingly, while we found SEC1A and KEU have functions during pollen germination and PT growth, SEC1B and KEU function redundantly during the late stages of pollen development leading to abortion in *sec1b keu* double mutant pollen (Figure 6h). The *sec1b keu* phenotype is reminiscent of the overexpression phenotype of another SYP-binding protein, *Arabidopsis thaliana* Tomosyn (AtTMS). AtTMS is an R-SNARE motif-containing protein that binds to several pollen-expressed SYP1s, inhibiting secretion. Overexpression of AtTMS leads to pollen developmental defects, specifically failure of intine deposition and disrupted cell plate formation during pollen mitosis I resulting in pollen abortion (Li et al., 2019). The loss of *sec1b* and *keu* may function analogously to the overexpression of AtTMS leading to their similar pollen phenotypes. However, we noted no disruption in pollen development in *sec1a* plants, even in the presence of *keu* (Figure 6g). The *sec1a* mutant phenotype was only apparent during PT elongation, suggesting a division of function between SEC1A and SEC1B, with SEC1B functioning earlier during pollen development and SEC1A functioning later during PT growth. An earlier role for SEC1B is also consistent with its expression during pollen development (Honys & Twell, 2004). However, this difference in function may also be explained by differences in binding partners or activities. While SYP124, SYP125 and

SYP131 are required for pollen germination and tube growth, they are not required for pollen development (Slane et al., 2017). Other Qa-SNAREs (KNOLLE, SYP112 and SYP132), however, are expressed during pollen development and may mediate earlier fusion events (Slane et al., 2017). There is precedence for binding preference among the SEC1 proteins. For example, KEU interacts with the open conformation of KNOLLE and SYP132, while SEC1B had a much weaker interaction with KNOLLE and a preference for SYP132 (Park et al., 2012; Karnahl et al., 2018). SEC1A has been shown to not bind to KNOLLE using an *in vitro* pull-down assay (Assaad et al., 2001).

Given *SEC1A*'s importance to PT growth in Arabidopsis, we hypothesized that *SEC1A* orthologs may have similar functions in other flowering plants. To explore this, we examined gene expression data available for pollen samples in four different species across broad evolutionary distances. Though expression data alone are not sufficient to conclude function in a given tissue, we found that in tomato and maize, a single *SEC1A*-like gene was highly expressed in pollen, while in rice, similar to Arabidopsis, more than one *SEC1*-like gene was expressed in pollen (Figures 6a,b and 7). Amborella contained only a single *SEC1*-like gene that was highly expressed in pollen (Figure 7e), possibly reflecting the high secretory demands of this cell type compared with the other samples in the data set.

EXPERIMENTAL PROCEDURES

Plant materials and growth conditions

Plants were grown under 16 h light/8 h dark cycles in a temperature-controlled growth room maintained at 23°C. Mutagenesis of the *hpat1* (SALK_120066) *hpat3* (SALK_04668) background, screening, sequencing and data analysis were carried out as previously described (Beuder et al., 2020). The *sec1b* (GABI-KAT_601G09) and *keule* (GABI-KAT_513H06) mutant alleles were provided by the Arabidopsis Biological Resource Center (Kleinboelting et al., 2012; Karnahl et al., 2018) and backcrossed to the Columbia-0 ecotype before analysis. Mutations were genotyped using the primers and restriction enzymes listed in Table S5. For direct sequencing of *SEC1A* in additional suppressor lines, the *SEC1A* coding sequence was amplified with the primers in Table S5 and sequenced by Sanger sequencing using the same primers by the University of Michigan DNA sequencing core. For seed counts, mature, pre-dehiscent siliques were cleared overnight in 70% ethanol then transferred to 50% glycerol for at least 2 days before counting using a dissecting microscope.

Cloning

To generate the genomic *SEC1A* construct used to rescue suppression, we amplified the *SEC1A* region from Columbia-0 in a single fragment including 664 bases of promoter region, the full coding region and 117 bp following the stop codon using the primers in Table S5 and Phusion® High-Fidelity DNA Polymerase. This fragment was recombined into pDONR221 using BP Clonase II™ (11789–020, ThermoFisher, Waltham, MA, USA) and transferred by recombination reaction into the plant binary expression vector pFAST-G01 (Shimada et al., 2010) using LR Clonase II™

(11791–020, ThermoFisher). Cloning of the C-terminal fusion of *SEC1A* with mNeonGreen was similarly done, except the *SEC1A* amplified region included only until the last coding codon and the entry clone was recombined into a previously described modified pFAST-R07 vector in which the GFP sequence was replaced with mNeonGreen (Beuder et al., 2020).

To generate the Lat52::mRuby2-RabA4b construct, the mRuby2 and RabA4b fragments were amplified from plasmid sources using the primers in Table S5. The two fragments were combined by Gibson assembly using the Gibson Assembly® Cloning Kit (E5510S, New England Biolabs, Ipswich, MA, USA), and the resulting merged fragment was recombined into pDONR221 P5-P2 using BP Clonase II™. This clone was then recombined along with a Lat52 promoter clone into the pFAST-G01 destination vector (Shimada et al., 2010; Beuder et al., 2020) using LR Clonase II™.

The resulting constructs were transformed into Arabidopsis of the appropriate genetic background by the floral dip method. To allow for quantitative comparisons, a single insertion event was crossed into all the necessary genetic backgrounds. Lat52::mRuby2-RabA4b was transformed into WT and then crossed into *sec1a-1*, and Lat52::GF(EXT3)P was transformed into *hpat1/3* and crossed into WT and *hpat1/3 sec1a-1* (Beuder et al., 2020).

Pollen assays and imaging

Pollen was germinated and grown on *in vitro* growth media as described previously (Beuder et al., 2020). Pollen was considered germinated if a PT the length of the pollen grain was visible, and tubes were considered branched if two morphologically distinct tips were visible. Sustained growth rate was measured by imaging a field of PTs at two times approximately 25 min apart. Lengths of individual tubes were measured at both times, and the difference in total length was taken and divided by the time interval between images. For imaging of PTs in the pistil, nearly mature buds of WT flowers were emasculated and allowed to mature for 24 h before pollination. Eight hours after pollination with WT or *sec1a-1* pollen, the pistils were collected and prepared as in Mori et al. (2006), with the exception that decolorized aniline blue was replaced with aniline blue fluorochrome (Biosupplies Australia). The prepared pistils were imaged on a Leica DM5500 compound microscope using a Leica DAP filter cube (excitation filter 405/10, emission filter 460/40).

The secretion index was measured as previously described (Beuder et al., 2020). For *SEC1A*-mNG imaging, transgenic pollen was grown on pollen growth media plates overlaid with a piece of cellophane. After 2 h of growth, PTs were transferred by dabbing the cellophane onto a slide with a drop of 4 µM FM4-64 in agarose-free liquid pollen growth media and slides were sealed with nail polish. PTs were imaged ~10 min after mounting. *SEC1A*-mNG was imaged on a Leica SP5 confocal microscope with a 488-nm excitation laser and emission range set at 494–575 nm, and FM4-64 was imaged with a 514-nm excitation laser and emission range set at 620–783 nm; a DD488/561 dichroic beam splitter and PMT detectors. For imaging during PT growth, the pollen was imaged directly on the pollen growth media plate on a Leica DM5500 compound microscope using a Leica GFP filter cube (excitation filter BP 470/40, emission filter BP 525/50).

For vesicle staining, WT, *hpat1/3* and *hpat1/3 sec1a-1* PTs were grown inside of imaging chambers as mentioned above. After 1 h, samples were incubated with 12 µM FM4-64 diluted in liquid germination medium for 15 min and imaged using the Leica Sp5 confocal microscope, using a 561-nm excitation laser, a DD488/561 dichroic beam splitter and PMT detector set to capture light at the 568–678-nm wavelength range. Images were captured in the

medial section for each PT ($N = 16$ for WT, $N = 20$ for *hpat1/3* and $N = 22$ for *hpat1/3 sec1-a1*). Laser intensity and gain settings were maintained constant during imaging of all genotypes, and fluorescence intensity was quantified using ImageJ.

The WT Col-0 or *sec1a-1* PTs expressing Lat52:mRuby2:RabA4b were germinated inside of an imaging chamber composed of a slide with a CoverWell silicone chamber (Grace Bio-Labs, GBL635051, Bend, OR, USA) filled with molten pollen growth media and solidified on a flat surface for ~1 min. Once solidified, pollen grains of either genotype were dusted on top of the medium and carefully covered with a coverslip. The samples were incubated for 50 min in a humid chamber at room temperature and imaged with a Leica SP8 laser-scanning confocal microscope, using a white light laser set to 550 nm excitation, notch filter set NF488/561/633 and HyD detector capturing signal in the 570–721-nm wavelength range. Images were captured in the medial section for each PT. Laser intensity and gain settings were maintained constant during imaging of both genotypes. Fluorescence intensity was quantified using ImageJ in both genotypes.

For anther sectioning and toluidine staining, flower buds and mature flowers of WT Col-0, *sec1b/+ keule/+* and *sec1a-1 keule/+* were fixed, embedded in LR-white resin, and sectioned following the protocol from Costa et al. (2013). Semi-thin sections (10 nm) were stained with 0.1% toluidine blue incubating the samples at 65°C for 30 sec and washing the excess stain with distilled water. Slides were mounted with Permount mounting medium (Fisher Scientific, Waltham, MA, USA) for long-term storage. The sectioned samples were then imaged using light microscopy (Leica, model DM5500B; camera Leica, model DFC365FX, Wetzlar, Germany). Developmental stages in the samples were determined based on the anther development description by Sanders et al. (1999).

Phylogeny and expression analysis

We identified SM proteins from tomato, rice and Amborella by BLAST sequence search using the Phytozome 12 database with the SEC1A protein sequence as query. The maize gene models were identified in the same way from the MaizeGDB database using the B73 FGS translations 5b.60 for RefGen_v2. A maximum parsimony phylogenetic tree was generated using 100 replicate bootstrap values using the Phylip 3.698 program suite with At3g22150 (AEF1) as an outgroup to root the tree (Felsenstein, 1989). The phylogeny was constructed using the full predicted protein coding sequences and, in the event that more than one transcript per gene was annotated, we took the one encoding the longest protein. We did not include SM members of the VSP33 family due to their weaker homology to SEC1.

Expression values of the SM homologs were gathered from published RNA-seq data (tomato – Lara-Mondragón & MacAlister, 2021; maize – Davidson et al., 2011; Amborella – Flores-Tornero et al., 2020; Arabidopsis – Loraine et al., 2013) or microarray data (rice – Wei et al., 2010; Arabidopsis – Klepikova et al., 2016), and a heatmap corresponding to the log₂ of the mean expression values per gene was plotted using the *heatmap* package in Rstudio. Species icons were generated using BioRender.

ACKNOWLEDGEMENTS

The authors would like to thank Erik Nielsen for providing a RabA4b containing plasmid and Gregg Sobocinski for imaging advice. This material is based upon work supported by the National Science Foundation under grant no. IOS-1755482. CLM receives fellowship funding from the Mexican Council of Science and Technology (CONACYT) (773973).

CONFLICT OF INTEREST

The authors declare no conflict of interest.

AUTHOR CONTRIBUTIONS

CAM carried out the original screen and genetic characterizations, designed the research plans and wrote the manuscript. SB analyzed whole-genome sequence data to identify candidate mutations, imaged the SEC1A-mNG reporter and measured the secretion index. CLM imaged the RabA4B reporter, analyzed pollen expression data and sectioned developing anthers. AD cloned the constructs.

DATA AVAILABILITY STATEMENT

Whole-genome sequence data for the *sec1a* suppressors can be found at the Sequence Read Archive (SRA) under project accession number: PRJNA808998. Additional data are available within the paper, the corresponding supplementary material or from the corresponding author on request.

SUPPORTING INFORMATION

Additional Supporting Information may be found in the online version of this article.

Figure S1. Rescue of suppression of the *hpat1/3* phenotype by the WT *SEC1A* genomic sequence.

Figure S2. Seed set is maintained in *sec1a* single mutants.

Figure S3. The impact of *keule* and *sec1b* on seed set and fertility.

Figure S4. The modified tomato *SEC1A* gene model.

Tables S1–S4 Complete lists of sequence variants passing filtering for the *hpat1/3* suppressors

Table S5. Primers used in this study

REFERENCES

- Alonso, J.M., Stepanova, A.N., Leisse, T.J., Kim, C.J. & Chen, H. (2003) Genome-wide insertional mutagenesis of Arabidopsis thaliana. *Science*, **301**, 653–657.
- Assaad, F.F., Huet, Y., Mayer, U. & Jürgens, G. (2001) The cytokinesis gene KEULE encodes a Sec1 protein that binds the syntaxin Knolle. *The Journal of Cell Biology*, **152**(3), 531–544.
- Assaad, F.F., Mayer, U., Wanner, G. & Jürgens, G. (1996) The KEULE gene is involved in cytokinesis in Arabidopsis. *Molecular and General Genetics*, **253**(3), 267–277.
- Baker, R.W. & Hughson, F.M. (2016) Chaperoning SNARE assembly and disassembly. *Nature Reviews Molecular Cell Biology*, **17**, 465–479.
- Bassham, D.C. & Raikhel, N.V. (1998) An Arabidopsis VPS45p homolog implicated in protein transport to the vacuole. *Plant Physiology*, **117**, 407–415.
- Bate, N. & Twell, D. (1998) Functional architecture of a late pollen promoter: pollen-specific transcription is developmentally regulated by multiple stage-specific and co-dependent activator elements. *Plant Molecular Biology*, **37**, 859–869.
- Beuder, S., Dorchak, A., Bhide, A., Moeller, S.R., Petersen, B.L. & CA, M.A. (2020) Exocyst mutants suppress pollen tube growth and cell wall structural defects of hydroxyproline O-arabinosyltransferase mutants. *The Plant Journal*, **103**, 1399–1419.
- Beuder, S. & MacAlister, C.A. (2020) Isolation and cloning of suppressor mutants with improved pollen fertility. In: Geitmann, A. (Ed.) *Pollen and Pollen Tube Biology: Methods and Protocols*. Springer Science+Business Media, LLC, part of Springer Nature, Berlin, Germany.
- Bloch, D., Pleskot, R., Pejchar, P., Potocký, M., Trpkosová, P., Cwiklik, L. et al. (2016) Exocyst SEC3 and phosphoinositides define sites of

- exocytosis in pollen tube initiation and growth. *Plant Physiology*, **172**, 980–1002.
- Borsics, T., Webb, D., Andeme-Ondzighi, C., Staehelin, L.A. & Christopher, D.A. (2006) The cyclic nucleotide-gated calmodulin-binding channel AtCNGC10 localizes to the plasma membrane and influences numerous growth responses and starch accumulation in *Arabidopsis thaliana*. *Planta*, **225**, 563–573.
- Bracher, A., Perrakis, A., Dresbach, T., Betz, H. & Weissenhorn, W. (2000) The X-ray crystal structure of neuronal Sec1 from squid sheds new light on the role of this protein in exocytosis. *Structure*, **8**, 685–694.
- Burkhardt, P., Stegmann, C.M., Cooper, B., Kloepper, T.H., Imig, C., Varoqueaux, F. et al. (2011) Primordial neurosecretory apparatus identified in the choanoflagellate *Monosiga brevicollis*. *Proceedings of the National Academy of Sciences of the United States of America*, **108**, 15264.
- Cannon, M.C., Terneus, K., Hall, Q., Tan, L., Wang, Y., Wegenhart, B.L. et al. (2008) Self-assembly of the plant cell wall requires an extensin scaffold. *Proceedings of the National Academy of Sciences of the United States of America*, **105**(6), 2226–2231.
- Carr, C.M., Grote, E., Munson, M., Hughson, F.M. & Novick, P.J. (1999) Sec1p binds to SNARE complexes and concentrates at sites of secretion. *The Journal of Cell Biology*, **146**, 333–344.
- Cascallares, M., Setzes, N., Marchetti, F., López, G.A., Distéfano, A.M., Cainzos, M. et al. (2020) A complex journey: cell wall remodeling, interactions, and integrity during pollen tube growth. *Frontiers in Plant Science*, **11**, 599247.
- Chen, Y., Dong, W., Tan, L., Held, M.A. & Kieliszewski, M.J. (2015) Arabinosylation plays a crucial role in extensin cross-linking in vitro. *Biochemistry Insights*, **8**(Suppl. 2), 1–13. <https://doi.org/10.4137/BCI.S31353>.
- Cole, R.A., Synek, L., Zarsky, V. & Fowler, J.E. (2005) SEC8, a subunit of the putative *Arabidopsis* exocyst complex, facilitates pollen germination and competitive pollen tube growth. *Plant Physiology*, **138**, 2005–2018.
- Costa, M., Pereira, A.M., Rudall, P.J. & Coimbra, S. (2013) Immunolocalization of arabinogalactan proteins (AGPs) in reproductive structures of an early-divergent angiosperm, *Trithuria* (Hydatellaceae). *Annals of Botany*, **111**(2), 183–190.
- Damineli, D.S.C., Portes, M.T. & Feijó, J.A. (2017) Oscillatory signatures underlie growth regimes in *Arabidopsis* pollen tubes: computational methods to estimate tip location, periodicity, and synchronization in growing cells. *Journal of Experimental Botany*, **68**(12), 3267–3281.
- Davidson, R.M., Hansey, C.N., Gowda, M., Childs, K.L., Lin, H., Vaillancourt, B. et al. (2011) Utility of RNA sequencing for analysis of maize reproductive transcriptomes. *The Plant Genome*, **4**(3), 191–203.
- Enami, K., Ichikawa, M., Uemura, T., Kutsuna, N., Hasazawa, S., Nakagawa, T. et al. (2008) Differential expression control and polarized distribution of plasma membrane-resident SYP1 SNAREs in *Arabidopsis thaliana*. *Plant and Cell Physiology*, **50**, 280–289.
- Felsenstein, J. (1989) PHYLIP - phylogeny inference package (version 3.2). *Cladistics*, **5**, 164–166.
- Flores-Tornero, M., Vogler, F., Mutwil, M., Potěšil, D., Ihnatová, I., Zdráhal, Z. et al. (2020) Transcriptomic and proteomic insights into *Amborella trichopoda* male gametophyte functions. *Plant Physiology*, **184**, 1640–1657.
- Grobei, M.A., Qeli, E., Brunner, E., Rehrauer, H., Zhang, R., Roschitzki, B. et al. (2009) Deterministic protein inference for shotgun proteomics data provides new insights into *Arabidopsis* pollen development and function. *Genome Research*, **19**(10), 1786–1800.
- Hála, M., Cole, R., Synek, L., Drdová, E., Pečenková, T., Nordheim, A. et al. (2008) Exocyst complex functions in plant cell growth in *Arabidopsis* and tobacco. *Plant Cell*, **20**, 1330–1345.
- Han, J., Pluhackova, K. & Böckmann, R.A. (2017) The multifaceted role of SNARE proteins in membrane fusion. *Frontiers in Physiology*, **8**, 5.
- Heppler, P.K. & Winship, L.J. (2014) The pollen tube clear zone: clues to the mechanism of polarized growth. *Journal of Integrative Plant Biology*, **57**(1), 79–92.
- Honys, D. & Twell, D. (2004) Transcriptome analysis of haploid male gametophyte development in *Arabidopsis*. *Genome Biology*, **5**(11), R85.
- Ichikawa, M., Iwano, M. & Sato, M.H. (2015) Nuclear membrane localization during pollen development and apex-focused polarity establishment of SYP124/125 during pollen germination in *Arabidopsis thaliana*. *Plant Reproduction*, **28**(3–4), 143–151.
- Karnahl, M., Park, M., Krause, C., Hiller, U., Mayer, U., Stierhof, Y.D. et al. (2018) Functional diversification of *Arabidopsis* SEC1-related SM proteins in cytokinetic and secretory membrane fusion. *Proceedings of the National Academy of Sciences of the United States of America*, **115**(24), 6309–6314.
- Karnik, R., Grefen, C., Bayne, R., Honsbein, A., Köhler, T., Kioumourtzoglou, D. et al. (2013) *Arabidopsis* Sec1/Munc18 protein SEC11 is a competitive and dynamic modulator of SNARE binding and SYP121-dependent vesicle traffic. *Plant Cell*, **25**(4), 1368–1382.
- Kelley, L.A., Mezulis, S., Yates, C.M., Wass, M.N. & Sternberg, M.J.E. (2015) The PyMol web portal for protein modeling, prediction and analysis. *Nature Protocols*, **10**, 845–858.
- Kleinboelting, N., Huep, G., Kloetgen, A., Viehoveer, P. & Weisshaar, B. (2012) GABI-Kat SimpleSearch: new features of the *Arabidopsis thaliana* T-DNA mutant database. *Nucleic Acids Research*, **40**, D1211–D1215.
- Klepikova, A.V., Kasianov, A.S., Gerasimov, E.S., Logacheva, M.D. & Pen, A.A. (2016) A high resolution map of the *Arabidopsis thaliana* developmental transcriptome based on RNA-seq profiling. *The Plant Journal*, **88**(6), 1058–1070.
- Lam, A.J., St-Pierre, F., Gong, Y., Marshall, J.D., Cranfill, P.J., Baird, M.A. et al. (2012) Improving FRET dynamic range with bright green and red fluorescent proteins. *Nature Methods*, **9**(10), 1005–1012.
- Lara-Mondragón, C.M. & MacAlister, C.A. (2021) Arabinogalactan glycoprotein dynamics during the progamic phase in the tomato pistil. *Plant Reproduction*, **34**, 131–148.
- Li, B., Li, Y., Liu, F., Tan, X., Rui, Q., Tong, Y. et al. (2019) Overexpressed Tomosyn binds syntaxins and blocks secretion during pollen development. *Plant Physiology*, **181**(3), 1114–1126.
- Li, Y., Tan, X., Wang, M., Li, B., Zhao, Y., Wu, C. et al. (2017) Exocyst subunit SEC3A marks the germination site and is essential for pollen germination in *Arabidopsis thaliana*. *Scientific Reports*, **7**, 40279.
- Loraine, A.E., McCormick, S., Estrada, A., Patel, K. & Qin, P. (2013) RNA-seq of *Arabidopsis* pollen uncovers novel transcription and alternative splicing. *Plant Physiology*, **162**, 1092–1109.
- MacAlister, C.A., Ortiz-Ramírez, C., Becker, J.D., Feijó, J.A. & Lippman, Z.B. (2016) Hydroxyproline O-arabinosyltransferase mutants oppositely alter tip growth in *Arabidopsis thaliana* and *Physcomitrella patens*. *Plant Journal*, **85**, 448–457.
- Marković, V., Čvrčková, F., Potocký, M., Kulich, I., Pejchar, P., Kollárová, E. et al. (2020) EXO70A2 is critical for exocyst complex function in pollen development. *Plant Physiology*, **184**(4), 1823–1839.
- Misura, K.M.S., Scheller, R.H. & Weis, W.I. (2000) Three-dimensional structure of the neuronal-Sec1-syntaxin 1a complex. *Nature*, **404**, 355–363.
- Mori, T., Kuroiwa, H., Higashiyama, T. & Kuroiwa, T. (2006) Generative cell specific 1 is essential for angiosperm fertilization. *Nature Cell Biology*, **8**(1), 64–71.
- Ogawa-Ohnishi, M., Matsushita, W. & Matsubayashi, Y. (2013) Identification of three hydroxyproline O-arabinosyltransferases in *Arabidopsis thaliana*. *Nature Chemical Biology*, **9**, 726–730.
- Park, M., Touihri, S., Müller, I., Mayer, U. & Jürgens, G. (2012) Sec1/Munc18 protein stabilizes fusion-competent syntaxin for membrane fusion in *Arabidopsis* cytokinesis. *Developmental Cell*, **22**, 989–1000.
- Parton, R.M., Fischer-Parton, S., Watahiki, M.K. & Trewaves, A.J. (2001) Dynamics of the apical vesicle accumulation and the rate of growth are related in individual pollen tubes. *Journal of Cell Science*, **114**(14), 2685–2695.
- Petersen, B.L., MacAlister, C.A. & Ulvskov, P. (2021) Plant protein O-Arabinosylation. *Frontiers in Plant Science*, **12**, 645219. <https://doi.org/10.3389/fpls.2021.645219>.
- Preuss, M.L., Serna, J., Falbel, T.G., Bednarek, S.Y. & Nielsen, E. (2004) The *Arabidopsis* Rab GTPase RabA4b localizes to the tips of growing root hair cells. *Plant Cell*, **16**, 1589–1603.
- Qin, Y., Leydon, A.R., Manziello, A., Pandey, R., Mount, D., Denic, S. et al. (2009) Penetration of the stigma and style elicits a novel transcriptome in pollen tubes, pointing to genes critical for growth in a pistil. *PLoS Genetics*, **5**(8), e1000621.
- Risselada, H.J. & Mayer, A. (2020) SNAREs, tethers and SM proteins: how to overcome the final barriers to membrane fusion? *Biochemical Journal*, **477**(1), 243–258.
- Rosso, M.G., Li, Y., Strizhov, N., Reiss, B., Dekker, K. & Weisshaar, B. (2003) An *Arabidopsis thaliana* T-DNA mutagenized population (GABI-Kat) for flanking sequence tag-based reverse genetics. *Plant Molecular Biology*, **53**, 247–259.

- Ruan, H., Li, J., Wang, T. & Ren, H. (2021) Secretory vesicles targeted to plasma membrane during pollen germination and tube growth. *Frontiers in Cell and Development Biology*, **8**, 615447.
- Rui, Q., Tan, X., Liu, F., Li, Y., Liu, X., Li, B. *et al.* (2021) Syntaxin of plants31 (SYP31) and SYP32 are essential for Golgi morphology maintenance and pollen development. *Plant Physiology*, **86**(1), 330–343.
- Sanderfoot, A.A., Assaad, F.F. & Raikhel, N.V. (2000) The *Arabidopsis thaliana* genome: an abundance of soluble N-ethylmaleimide-sensitive factor adaptor protein receptors. *Plant Physiology*, **124**, 1558–1569.
- Sanderfoot, A.A., Pilgrim, M., Adam, L. & Raikhel, N.V. (2001) Disruption of individual members of Arabidopsis Syntaxin gene families indicates each has essential functions. *Plant Cell*, **13**, 659–666.
- Sanders, P.M., Bui, A.Q., Weterings, K., McIntire, K.N., Hsu, Y.-C., Lee, P.Y. *et al.* (1999) Anther developmental defects in Arabidopsis thaliana male-sterile mutants. *Sexual Plant Reproduction*, **11**(6), 297–322.
- Sessions, A., Burke, E., Presting, G., Aux, G., McElver, J., Patton, D. *et al.* (2002) A high-throughput arabidopsis reverse genetics system. *The Plant Cell*, **14**, 2985–2994.
- Shimada, T.L., Shimada, T. & Hara-Nishimura, I. (2010) A rapid and non-destructive screenable marker, FAST, for identifying transformed seeds of Arabidopsis thaliana. *The Plant Journal*, **61**, 519–528.
- Silva, P.A., Ul-Rehman, R., Rato, C., Sanebastiano, G.D. & Malho, R. (2010) Asymmetric localization of Arabidopsis SYP124 syntaxin at the pollen tube apical and sub-apical zones is involved in tip growth. *BMC Plant Biology*, **10**, 179.
- Slane, D., Reichardt, I., Kasmi, F.E., Bayer, M. & Jürgens, G. (2017) Evolutionarily diverse SYP1 Qa-SNAREs jointly sustain pollen tube growth in Arabidopsis. *The Plant Journal*, **92**(3), 375–385.
- Sogaard, M., Tani, K., Ye, R.R., Geromanos, S., Tempst, P., Kirchhausen, T. *et al.* (1994) A Rab protein is required for the assembly of SNARE complexes in the docking of transport vesicles. *Cell*, **78**(6), 937–948.
- Sogawa, A., Takahashi, I., Kyo, M., Imaizumi-Anraku, H., Tajima, S. & Nomura, M. (2020) Requirements of Qa-SNARE LjSYP132s for nodulation and seed development in lotus japonicas. *Plant and Cell Physiology*, **61**(10), 1750–1759.
- Südhof, T.C. & Rothman, J.E. (2009) Membrane fusion: grappling with SNARE and SM proteins. *Science*, **323**(5913), 474–477. <https://doi.org/10.1126/science.1161748>.
- Ul-Rehman, R., Silva, P.A. & Malho, R. (2011) Localization of Arabidopsis SYP125 syntaxin in the plasma membrane sub-apical and distal zones of growing pollen tubes. *Plant Signaling & Behavior*, **6**(5), 665–670.
- Wei, L.Q., Zu, W.Y., Deng, Z.Y., Su, Z., Xue, Y. & Wang, T. (2010) Genome-scale analysis and comparison of gene expression profiles in developing and germinated pollen in *Oryza sativa*. *BMC Genomics*, **11**, 338.
- Woody, S.T., Austin-Phillips, S. & Amasino, R.M. (2007) The WiscDsLox T-DNA collection: an Arabidopsis community resource generated by using an improved high-throughput T-DNA sequencing pipeline. *Journal of Plant Research*, **120**, 157–165.
- Zouhar, J., Rojo, E. & Bassham, D.C. (2009) AtVPS45 is a positive regulator of the SYP41/SYP61/VT112 SNARE complex involved in trafficking of vacuolar cargo. *Plant Physiology*, **149**(4), 1668–1678.